

# Cyclodehydrogenation Reactions to Cyclopentafused Polycyclic Aromatic Hydrocarbons

Angela Violi\*

Department of Mechanical Engineering, University of Michigan, Ann Arbor, MI 48109

Received: May 8, 2005

B3LYP/6-31G(d,p) electronic structure calculations are employed to elucidate the reaction mechanisms for the conversion of the alternant  $C_{18}H_{12}$  polycyclic aromatic hydrocarbon benzo[*c*]phenanthrene into the nonalternant  $C_{18}H_{10}$  PAHs cyclopenta[*cd*]pyrene and benzo[*ghi*]fluoranthene. Isomerization reactions such as 5/6-ring switching and hydrogen atom scrambling are analyzed. Bay region chemistry, involving the rupture of one benzene ring followed by the formation of a new five-membered ring, is also studied, together with the mechanism for the formation of an aryne. The rearrangement of the latter yields annelated cyclopentadienylidene carbene, which is then trapped intramolecularly.

## Introduction

Polycyclic aromatic hydrocarbons (PAHs) containing fully unsaturated five-membered rings as integral components of their trigonal carbon networks (CP-PAHs) have attracted considerable attention in different fields.<sup>1–3</sup> Some of these nonalternant hydrocarbons exhibit unusual photophysical behavior<sup>4,5</sup> and biological activity.<sup>6</sup> Toxicity studies provide strong evidence that CP-PAHs are primarily responsible for the genotoxicity of combustion mixtures.<sup>7–9</sup>

Relative to other PAHs, CP-PAHs demonstrate a greater facility to undergo certain kinds of reactions, such as isomerization involving intramolecular rearrangement.<sup>7,10</sup> This is due to the fact that fusion of the cyclopenta ring alters the electronic properties of the PAH, as demonstrated by differences in the resonance energy<sup>11</sup> and measured differences in ultraviolet–visible (UV–vis) absorption<sup>12</sup> and fluorescence.<sup>4,5</sup> The presence of five- and six-membered rings may also provide the structural property of nonplanarity to CP-PAHs. Bowl-shaped CP-PAHs such as corannulene constitute building blocks for fullerenes.<sup>13–17</sup>

Recently, CP-PAHs have been widely found in combustion systems (e.g., Lafleur et al.<sup>18</sup>); they have been observed as pyrolysis products of anthracene,<sup>19,20</sup> pyrene,<sup>21</sup> and benzene<sup>22</sup> and as combustion products of benzene,<sup>23</sup> ethylene, and ethylene–naphthalene<sup>24</sup> mixtures. Wornat et al.<sup>25</sup> pyrolyzed brown coal and, through the analysis of the product tar, identified several different CP-PAHs. Consequently, the elucidation of CP-PAH formation processes under high-temperature conditions is an important research topic.

According to Badger's free radical mechanism,<sup>26,27</sup> simple aromatic hydrocarbons first lose hydrogen through a C–H bond cleavage, producing aryl radicals. Recombination of these radicals yields biaryls, which in turn are subject to further dehydrogenation. The energy of the C–H bond in simple PAHs is determined mostly by steric effects.<sup>28</sup> Consequently, the loss of hydrogen is expected to occur preferentially at sterically congested sites, where new C–C bonds may readily form, implying the propensity of aryls to undergo, whenever possible, cyclodehydrogenation rather than dehydrogenative polymerization.

Little is known about the basic mechanism of thermally induced cyclodehydrogenation reactions. Two hydrogen atoms are lost, and a new ring is created by the formation of a new transannular C–C bond. The details concerning the order of the steps and the nature of the reactive intermediates are still missing, and most of the reaction mechanisms for cyclodehydrogenation do not account for the presence of CP-PAHs.

The importance of cyclodehydrogenation reactions and interconversions of PAHs to combustion chemistry, combined with the lack of definite experimental evidence for the mechanisms, has emphasized the need to carry out a comprehensive state-of-the-art electronic structure study of cyclodehydrogenation of benzo[*c*]phenanthrene (**1**) (Figure 1). This compound has been proposed to play an important role in competing PAH growth pathways, i.e., the buildup of planar versus nonplanar CP-PAHs.<sup>29,30</sup> Thermolysis of **1** produces not only benzo[*ghi*]fluoranthene but also cyclopenta[*cd*]pyrene. Evidence for the viability of this process has been obtained from flash vacuum thermolysis (FVT) experiments.<sup>31–36</sup> These reactions are believed to proceed through several stages,<sup>29,37</sup> including dehydrogenation as well as rearrangements such as intramolecular trapping, H scrambling, and five- to six-membered interconversion.<sup>9,38–40</sup>

A detailed analysis of these reactions together with the elucidation of efficient high-temperature routes is reported in this paper. After the first two sections, which describe the formation pathways from benzo[*c*]phenanthrene to benzo[*ghi*]fluoranthene and cyclopenta[*cd*]pyrene, respectively, the interconversion of the latter two nonalternant  $C_{18}H_{10}$  PAHs is reported. Reaction rates are computed for the pathways analyzed together with the thermodynamic data of all the intermediates involved in the reaction steps.

Since benzo[*c*]phenanthrene may be regarded as a rigid analogue of 1-phenylnaphthalene, and Cioslowsky et al.<sup>41</sup> reported a detailed analysis of its thermally induced cyclodehydrogenation, some of the results presented in this study for benzo[*c*]phenanthrene are compared with those obtained for 1-phenylnaphthalene.

## Details of the Calculations

All calculations in this study were carried out with the GAUSSIAN G03 suite of programs.<sup>42</sup> Geometries of all species

\* E-mail: violi@eng.utah.edu; until Jan 2006 at the University of Utah, Department of Chemical Engineering and Department of Chemistry.

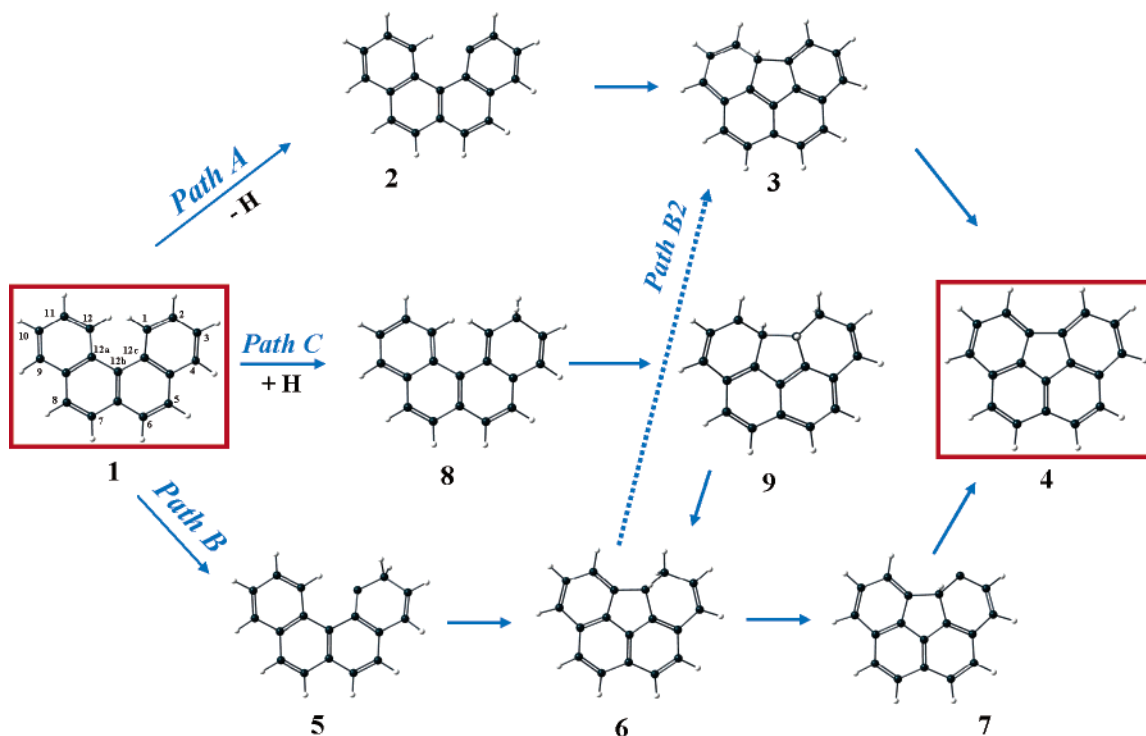


**Figure 1.** Reaction pathways A–C.

under study were fully optimized, and their vibrational frequencies were calculated. All the predictions of reaction energetics and barriers cited in the following text and figures pertain to energies at the B3LYP/6-31G(d,p) level of theory.

To assess the suitability of the B3LYP/6-31G(d,p) level of theory for studies of reactions involving aryl radicals, arynes, and carbenes, we performed comparisons with experimental data available for compounds that belong to those classes. Thus, the B3LYP/6-31G(d,p) C–H bond dissociation energy (BDE) of benzene equals 110.17 kcal/mol at  $T = 0$  K, in agreement with the recent experimental values of  $109.8 \pm 0.8$  kcal/mol<sup>43</sup> and  $112.0 \pm 0.6$  kcal/mol.<sup>44</sup>

Benchmark MP2/6-311G\*\*, QCISD/6-311G\*\*, and CCSD(T)/6-311G\*\* calculations for 1,2-didehydrogenation of benzene ( $C_6H_6 \rightarrow C_6H_4 + H_2$ ) produce values of 86.1, 91.2, and 86.8 kcal/mol, respectively,<sup>45</sup> whereas the B3LYP/6-31G(d,p) calculations yield 91 kcal/mol. All these figures agree quite well with the recent experimental estimate of  $86.9 \pm 3.0$  kcal/mol (at  $T = 298$  K).<sup>46</sup> Impressive agreement is observed between the B3LYP/6-31G(d,p) predictions for the energy of the benzyne  $\rightarrow$  cyclopentadienylidene carbene isomerization, 29.3 kcal/mol, and the CCSD(T)/6-311G\*\* predictions, which give the same value, 29.3 kcal/mol.<sup>43</sup> Also the B3LYP/6-31G(d,p) energy of the  $H_2C=C: \rightarrow HC\equiv CH$  rearrangement,  $-39.7$  kcal/mol, is close to the experimental value of  $-43 \pm 2$  kcal/mol.

In summary, the CCSD(T)/6-31G\*\* energetics of the species involved in both the 1,2-didehydrogenation of benzene and the 1,2-benzyne are accurately reproduced by the B3LYP/6-31G(d,p) method, warranting its use in studies of analogous reactions of larger PAHs.

The energies and barriers quoted in this paper pertain to  $T = 0$  K and include zero-point energies.

## Reaction Pathways

**Benzo[ghi]fluoranthene Formation.** Figure 1 shows three possible pathways for the conversion of benzo[c]phenanthrene to benzo[ghi]fluoranthene.

**Pathway A.** The cyclodehydrogenation of 1 may proceed through the initial abstraction of hydrogen from C1 to produce radical 2. The removal of hydrogen lessens the steric congestion present in the parent aryl: the inter-ring dihedral angle in 2 is  $0^\circ$ , whereas that in 1 is  $18^\circ$ . As already mentioned, since the energy of the homolytic C–H bond cleavage in the PAH is governed by steric rather than electronic effects, hydrogen abstraction from position 1 is favored over that from the others by about 7 kcal/mol.

Radical 2 is predicted to readily undergo intramolecular ring closure to intermediate 3. The transition state of this reaction is found to be quite early, with the length of the C–C bond under formation amounting to ca. 2.17 Å in the transition state. The partial loss of aromaticity that accompanies the ring closure offsets the energy gains due to formation of the C–C bond, resulting in a predicted reaction energy of  $-7.6$  kcal/mol.

C–H bond cleavage completes the pathway from 1 to benzo[ghi]fluoranthene (4), where the aromaticity is restored upon the removal of hydrogen. This process involves a transition state energy of 25.3 kcal/mol. The present calculation places the products  $4 + H_2$  15 kcal/mol above the reactant. Thus, once formed, compound 2 is rapidly converted to a pericondensed PAH and H in a two-step process with low energy barriers.

**Pathway B.** The formation of benzo[ghi]fluoranthene can also progress through a 1,2-shift of hydrogen out of the cove region to the adjacent carbon to produce radical 5. The energy barrier for this reaction was identified to be 81 kcal/mol. This type of scrambling of hydrogen atoms represents an important thermal reaction for PAHs.<sup>47</sup> In 5, the hydrogen 1,5-shift between the atoms C1 and C12 is facilitated by their proximity. As a consequence, a further H migration from C12 leads to compound 6, which is placed 18 kcal/mol in energy above the reactant 1. The predicted reaction barrier for this reaction is 11.8 kcal/mol. The elimination of the two hydrogens bonded to the  $sp^3$  C2 produces intermediate 7, and the further H migration from the C1 to C2 leads to benzo[ghi]fluoranthene. The reaction barriers involved in these last two steps are 90.15 kcal/mol for

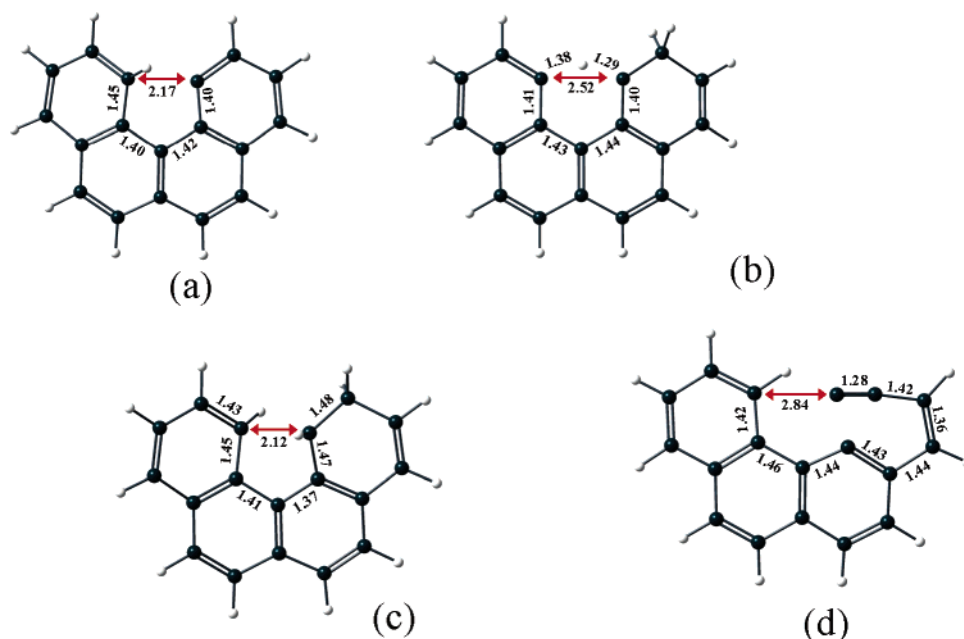


**Figure 2.** Selected C–C and C–H bond lengths (Å) in the transition states of the intramolecular ring closures  $2 \rightarrow 3$  (a),  $5 \rightarrow 6$  (b),  $8 \rightarrow 9$  (c), and  $10 \rightarrow 11$  (d).

the  $6 \rightarrow 7$  transition and 0.2 kcal/mol for the  $7 \rightarrow 4$  transition, respectively. This indicates that, once **7** is formed, it is rapidly converted to benzo[ghi]fluoranthene. As an alternative, from intermediate **6** the reaction can proceed through H abstraction of one of the two hydrogens bonded to C2 to produce radical **3** (dotted line). The barrier energy for this H abstraction is 18.4 kcal/mol. From intermediate **3** the reaction route is similar to pathway A, and benzo[ghi]fluoranthene is formed through C–H bond cleavage in intermediate **3**.

The 1,2-elimination of molecular hydrogen from compound **6** to directly produce compound **4** is forbidden by orbital symmetry.

**Pathway C.** The conversion of benzo[c]phenanthrene to benzo[ghi]fluoranthene can also be initiated by the addition of a hydrogen atom to the 2-position of benzo[c]phenanthrene, producing intermediate **8**. Whereas abstraction is close to thermoneutral when the abstracting reagent is a hydrogen atom, the addition of a hydrogen atom to benzo[c]phenanthrene is quite exothermic,  $-26.95$  kcal/mol, and the activation energy is 2.84 kcal/mol. The resulting radical can then undergo conrotatory ring closure, forming a trans-ring junction (compound **9**) that then loses a hydrogen atom to give intermediate **6**. This type of electrocyclic reaction involves the exchange of  $\pi$ -bonds for ring-closing  $\sigma$ -bonds. Ring closure occurs when both orbitals rotate in the same direction to achieve overlap. In other words, conrotatory ring closure occurs when the top lobe of one orbital has the same phase as the bottom lobe of the other orbital involved in forming the  $\sigma$ -bond. At this point, the reaction pathway can progress either in the same way as pathway B, forming first intermediate **7** and then benzo[ghi]fluoranthene through H migration, or as in pathway B2, producing first radical **3** and then benzo[ghi]fluoranthene.

Figure 2 reports the optimized structures of the transition states for the reactions  $2 \rightarrow 3$  (Figure 2a),  $5 \rightarrow 6$  (Figure 2b), and  $8 \rightarrow 9$  (Figure 2c).

Figure 3 shows the B3LYP/6-31G(d,p) energy profiles for pathways A–C.

Pathways A and C are facilitated by the presence of radicals in the environment, and they represent the principal sources for

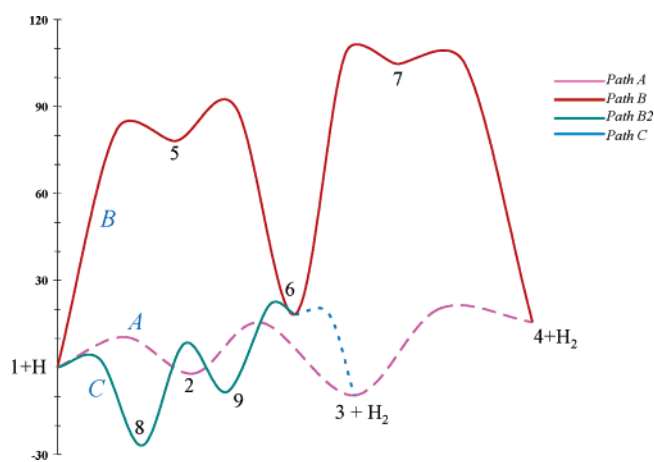


**Figure 3.** Energy profiles for pathways A–C.

the production of benzo[ghi]fluoranthene in the presence of H atoms.

In a H-poor environment pathways A and B become competitive. The initial dehydrogenation step to produce compound **2** in pathway A requires the elimination of a H atom from **1**, and the bond dissociation energy is found to be 103.2 kcal/mol. This result is similar to that obtained by Cioslowski et al.,<sup>39</sup> who identified the energy for the H loss from 1-phenyl-naphthalene at the BLYP/6-31G\*\* level to be around 105 kcal/mol. As a consequence, in a H-poor environment the first steps involved in pathways A and B both have significant energy barriers (the transition energy for  $1 \rightarrow 5$  is 81 kcal/mol), and they can both contribute to the formation of benzo[ghi]fluoranthene.

**Cyclopenta[cd]pyrene Formation.** Figure 4 shows reaction pathway D for the conversion of benzo[c]phenanthrene to cyclopenta[cd]pyrene.

**Pathway D.** The formation of cyclopenta[cd]pyrene from benzo[c]phenanthrene can be rationalized by invoking the benzyne–cyclopentadienyliidene rearrangement, i.e., the formation of 1,2-dehydrobenzo[c]phenanthrene via homolysis of a peri aryl C–H bond,<sup>48</sup> followed by loss of a vicinal

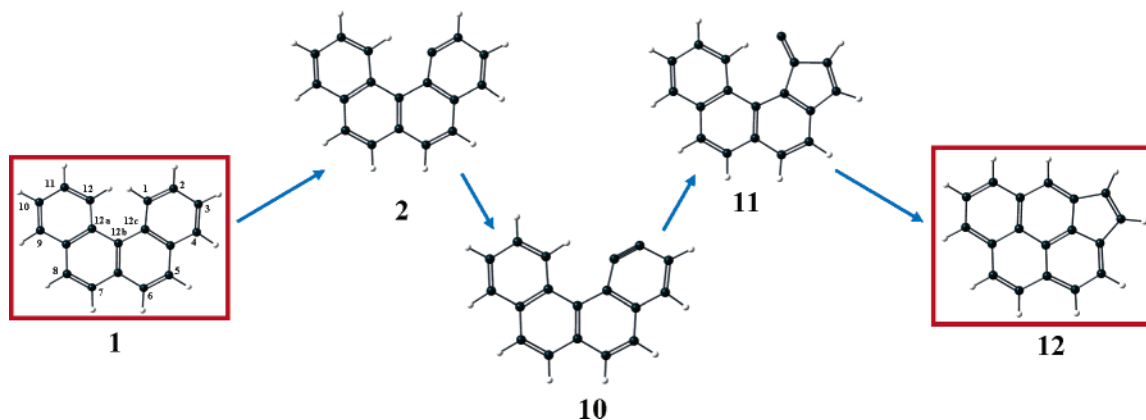


Figure 4. Reaction pathway D.

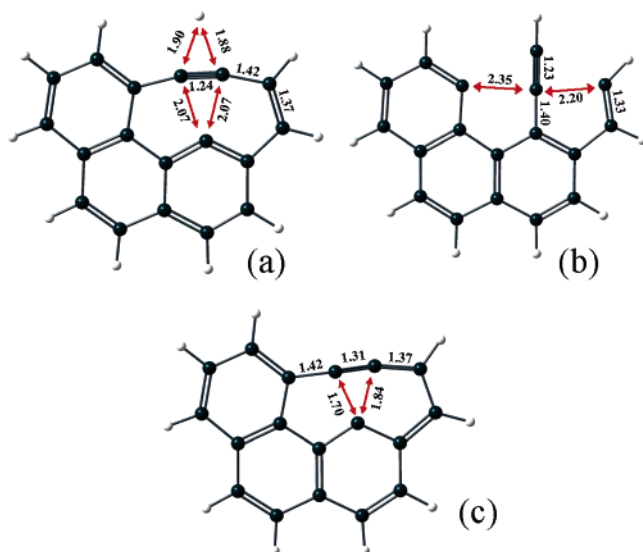


Figure 5. Optimized structures for the transition states of the reaction pathways E (a), F (b), and G (c).

hydrogen. When exposed to radicals, for example, in flame conditions, the aryl radical **2** may undergo further dehydrogenation, forming compound **10**, where the H bonded to C2 has been removed. The energy barrier for the H abstraction from intermediate **2** by a H atom is 13.6 kcal/mol at the B3LYP/6-31G(d,p) level of theory.

Benzyne benzologue **10** will produce its carbene isomer **11** (Figure 4), which then gives cyclopenta[*cd*]pyrene (**12**) via intramolecular trapping (C–H insertion).

The energy barrier for the reaction  $\mathbf{10} \rightarrow \mathbf{11}$  is 41.3 kcal/mol. Only the singlet electronic state was considered for compound **11** (singlet,  $-691.82$  hartrees; triplet,  $-691.76$  hartrees; quintet,  $-691.69$  hartrees) in agreement with recent electronic structure calculations on cyclopentadienylidene-carbene.<sup>49</sup> The reaction energy for  $\mathbf{10} \rightarrow \mathbf{11}$  is almost the same as that of the benzyne  $\rightarrow$  cyclopentadienylidene-carbene rearrangement (24.28 kcal/mol vs 29.28 kcal/mol), also in agreement with the results reported by Cioslowski et al.<sup>39</sup> The computed lengths of the analogous C–C bonds in **11** and cyclopentadienylidene-carbene are quite similar, indicating the lack of significant conjugation between cyclopentadiene and 6-ring moieties. The highly exothermic cyclization, which involves formation of a C–C bond concurrent with a hydrogen 1,2-shift, is predicted to possess an activation enthalpy of only 7.6 kcal/mol. The products cyclopenta[*cd*]pyrene + 2H<sub>2</sub> lie 94 kcal/mol below the reactants **1** + 2H. The optimized structure for the transition state of  $\mathbf{10} \rightarrow \mathbf{11}$  is reported in Figure 2d.

In a H-poor environment, the benzyne pathway to form intermediate **10** requires significant energy since the dissociation bond energy to form **10** from radical **2** is computed to be 86.2 kcal/mol.

**From Benzo[*ghi*]fluoranthene to Cyclopenta[*cd*]pyrene.** The conversion of benzo[*ghi*]fluoranthene to cyclopenta[*cd*]pyrene is an example of the Stone–Wales rearrangement, which involves the transposition of two sp<sup>2</sup>-hybridized carbon atoms within a framework of other sp<sup>2</sup>-hybridized atoms. Mechanisms for the Stone–Wales rearrangement have been extensively discussed,<sup>50,51</sup> and it has also recently been pointed out that radical-promoted mechanisms can be energetically very favorable.<sup>52</sup> Below we report reaction pathways involving unimolecular and bimolecular reactions for the interconversion of benzo[*ghi*]fluoranthene into cyclopenta[*cd*]pyrene.

**Unimolecular Reactions.** Since the original work of Scott and Roelofs<sup>10</sup> on the 5/6-ring interconversion, many examples have been found<sup>29,30,35,38,53,54</sup> and the process appears to be common among CP-PAHs at high temperatures in the gas phase. The ring-contraction/ring-expansion sequence, i.e., the exchange of five- and six-membered rings, can be achieved by breaking one C–H bond and one C–C bond while forming one C–H bond and one C–C bond<sup>10</sup> (pathway E). Figure 5a reports the optimized structures for this transition state. In a similar way, a four-centered reaction involving concurrent breaking of two C–C bonds (C2–C3 and C12–C1) and forming of two C–C bonds can be considered for the production of cyclopenta[*cd*]pyrene from benzo[*ghi*]fluoranthene (pathway F). The energy barriers for pathways E and F are 161.6 and 163.3 kcal/mol, respectively. Figure 5b reports the optimized structures for the transition states of pathway F.

**Bimolecular Reactions.** In the presence of H atoms, benzo[*ghi*]fluoranthene can undergo H abstraction to produce intermediate **15** and H<sub>2</sub> as shown in Figure 6 (pathway G).

The energy barrier and reaction energy for the reaction  $\mathbf{4} \rightarrow \mathbf{13}$  are 9.9 and 4.8 kcal/mol, respectively. The following ring-opening/ring-expansion reaction leading to intermediate **14** has an energy barrier of 49.0 kcal/mol. The transition state for the reaction  $\mathbf{13} \rightarrow \mathbf{14}$  is reported in Figure 5c. H atoms from the gas phase can then add to the radical on **14** to produce cyclopenta[*cd*]pyrene. The reaction energy for  $\mathbf{14} + \text{H} \rightarrow \mathbf{12}$  with zero-point energy correction is  $-110$  kcal/mol.

Pathway H in Figure 6 represents another possibility for the interconversion of benzo[*ghi*]fluoranthene to cyclopenta[*cd*]pyrene by a radical-promoted route. H atom addition to compound **4** produces radical **3**—the same as in pathway A—which can then undergo ring closure to a cyclopropane (**15**), initiating the rearrangement. The energy barrier for the reaction

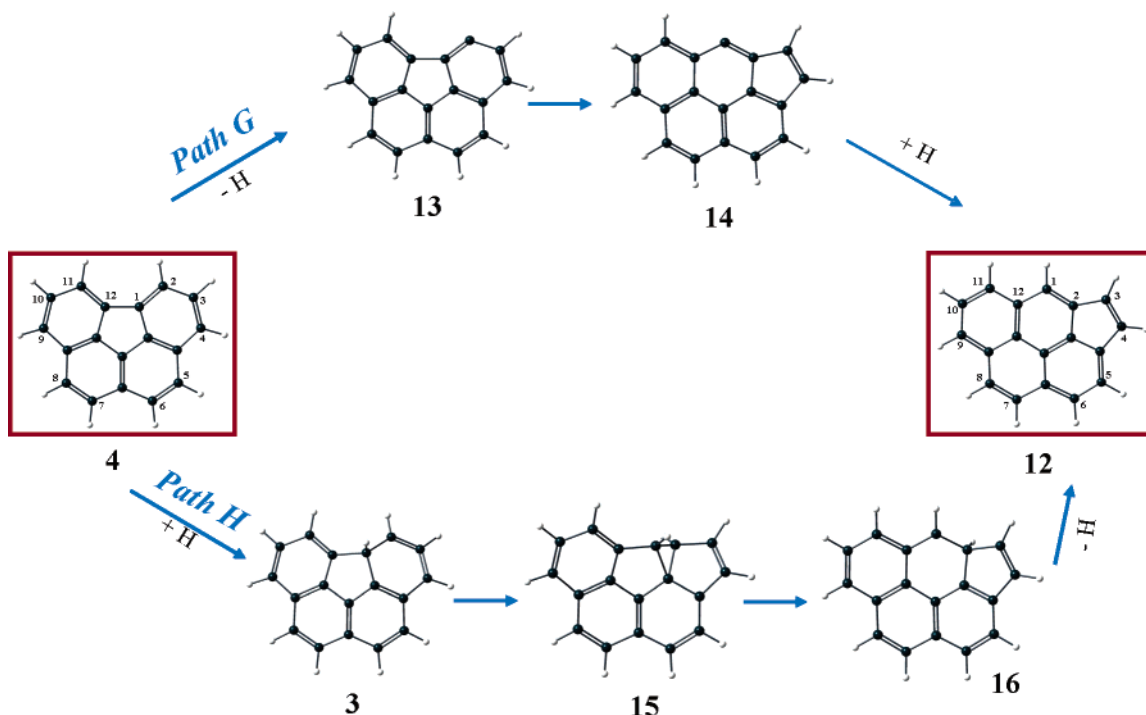


Figure 6. Reaction pathways G and H for the interconversion of benzo[ghi]fluoranthene to cyclopenta[cd]pyrene.

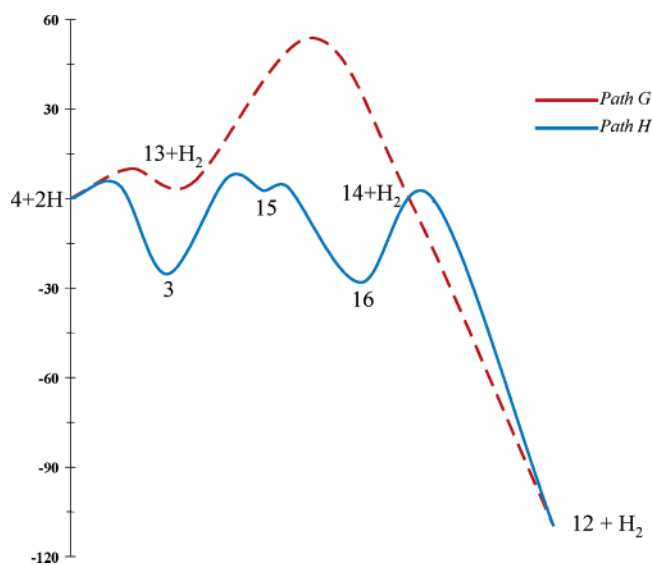


Figure 7. Energy profiles for pathways G and H.

$3 \rightarrow 15$  is 32.3 kcal/mol. The 5/6-ring interconversion proceeds then through the formation of intermediate **16**, where the C1–C12c bond is broken and the six-membered ring is formed. The barrier for the reaction  $15 \rightarrow 16$  is 1.15 kcal/mol. Further H removal from C2 leads to cyclopenta[cd]pyrene.

Figure 7 shows the B3LYP/6-31G(d,p) energy profiles for pathways G and H.

DFT calculations are used to compute the reaction rates for the pathways described above. The enthalpies and entropies are treated with conventional transition-state theory to calculate Arrhenius preexponential factors and energies of activation that result in high-pressure-limit rate constants ( $k_\infty$ ) as functions of temperature. Nonlinear Arrhenius effects resulting from changes in the thermochemical properties of the respective transition state relative to those of its adduct with temperature are incorporated using a two-parameter Arrhenius preexponential factor ( $A$ ,  $n$ ) in  $AT^n$ . Rate constants were calculated from the transition-state theory, using TheRate (Theoretical Rates) code<sup>55</sup> at the CSEO

TABLE 1: Reaction Rates for Pathways A–H

reaction	$A^a$	$n$	$E$
Pathways A–E			
$1 + H \rightarrow 2 + H_2$	7.25E+07	1.76	9.69E+03
$1 \rightarrow 2 + H$	2.76E+09	1.44	1.19E+05
$2 \rightarrow 3$	3.86E+11	0.21	1.77E+04
$3 \rightarrow 4 + H$	5.75E+10	0.93	3.04E+04
$1 \rightarrow 5$	9.70E+11	0.64	8.30E+04
$5 \rightarrow 6$	2.18E+11	0.37	1.18E+04
$1 + H \rightarrow 8$	6.54E+08	1.5	1.82E+03
$8 \rightarrow 9$	5.61E+11	0.21	1.77E+04
$9 \rightarrow 6 + H$	4.56E+10	0.95	3.04E+04
$2 + H \rightarrow 10 + H_2$	3.52E+08	1.83	1.50E+04
$2 \rightarrow 10 + H$	1.23E+10	1.41	8.52E+04
$10 \rightarrow 11$	1.04E+12	0.41	4.21E+04
$11 \rightarrow 12$	7.81E+11	0.18	7.64E+03
Pathways E–H			
$4 \rightarrow 12$	3.33E+10	1.65	1.64E+05
$4 + H \rightarrow 13 + H_2$	1.74E+08	1.74	9.37E+03
$13 \rightarrow 14$	4.96E+11	0.755	5.0E+04
$14 + H \rightarrow 12$	2.33E+08	1.39	-1.95E+03
$3 \rightarrow 15$	1.64E+12	0.38	1.62E+04
$15 \rightarrow 16$	8.15E+12	0.05	1.61E+03
$16 \rightarrow 12 + H$	6.90E+10	0.97	1.44E+04

<sup>a</sup> Arrhenius format  $k = AT^n \exp(-E/RT)$ , units  $\text{cm}^3/(\text{mol K s})$ .

online resource (<http://www.cseo.net>). The transmission coefficients which account for the quantum mechanical tunneling effect were calculated using the Eckart method.<sup>56</sup>

The thermal rate coefficient is expressed as

$$k(T) = \kappa(T) \sigma \frac{k_B T}{h} \frac{Q^\ddagger(T)}{\Phi^R(T)} e^{-\Delta V^\ddagger/k_B T}$$

where  $\kappa$  is the transmission coefficient accounting for the quantum mechanical tunneling effects,  $\sigma$  is the reaction symmetry number,  $Q^\ddagger$  and  $\Phi^R$  are the total partition functions (per unit volume) of the transition state and reactant, respectively,  $\Delta V^\ddagger$  is the classical barrier height,  $T$  is the temperature, and  $k_B$  and  $h$  are the Boltzmann and Planck constants, respectively.

**TABLE 2: Thermodynamic Data of Species Considered in the Present Work ( $C_p$ , cal mol<sup>-1</sup> K<sup>-1</sup>)**

species	$C_p$ (300 K)	$C_p$ (500 K)	$C_p$ (700 K)	$C_p$ (900 K)	$C_p$ (1100 K)	$C_p$ (1300 K)	$C_p$ (1500 K)
1	5.441E+01	8.956E+01	1.127E+02	1.279E+02	1.384E+02	1.460E+02	1.516E+02
2	5.421E+01	8.812E+01	1.103E+02	1.248E+02	1.348E+02	1.419E+02	1.472E+02
3	5.310E+01	8.776E+01	1.103E+02	1.249E+02	1.349E+02	1.421E+02	1.473E+02
4	5.114E+01	8.462E+01	1.065E+02	1.206E+02	1.303E+02	1.372E+02	1.422E+02
5	5.623E+01	9.097E+01	1.138E+02	1.288E+02	1.392E+02	1.466E+02	1.521E+02
6	5.336E+01	8.880E+01	1.123E+02	1.278E+02	1.384E+02	1.461E+02	1.517E+02
7	5.265E+01	8.600E+01	1.076E+02	1.216E+02	1.311E+02	1.378E+02	1.427E+02
8	5.661E+01	9.256E+01	1.164E+02	1.320E+02	1.429E+02	1.508E+02	1.566E+02
9	5.523E+01	9.181E+01	1.160E+02	1.319E+02	1.430E+02	1.509E+02	1.567E+02
10	5.403E+01	8.636E+01	1.075E+02	1.213E+02	1.307E+02	1.375E+02	1.424E+02
11	5.478E+01	8.709E+01	1.081E+02	1.218E+02	1.312E+02	1.379E+02	1.428E+02
12	5.143E+01	8.488E+01	1.067E+02	1.208E+02	1.304E+02	1.373E+02	1.423E+02
13	5.063E+01	8.296E+01	1.039E+02	1.174E+02	1.265E+02	1.330E+02	1.377E+02
14	5.086E+01	8.317E+01	1.041E+02	1.175E+02	1.266E+02	1.330E+02	1.377E+02
15	5.336E+01	8.845E+01	1.109E+02	1.253E+02	1.352E+02	1.422E+02	1.474E+02
16	5.337E+01	8.803E+01	1.105E+02	1.250E+02	1.350E+02	1.421E+02	1.473E+02

Table 1 reports the computed reaction rates for the pathways analyzed above.

### Reaction Mechanism and Kinetic Modeling

The reaction pathways identified above were implemented in a Chemkin-type kinetic mechanism to simulate a high- $T$  (1500 K) pyrolytic environment, using the SENKIN program of the CHEMKIN package,<sup>57,58</sup> which predicts the time-dependent chemical kinetics behavior of a homogeneous gas mixture in a closed system. The mechanism includes microscopic reversibility for all the elementary reactions considered. Table 2 reports the computed thermodynamic data for the species involved in pathways A–H. The values agree very well with data previously reported in the literature for polycyclic aromatic hydrocarbons containing five-membered rings.<sup>59</sup> Two cases were analyzed: the first one using pure benzo[*c*]phenanthrene as reactant and the second one with benzo[*c*]phenanthrene, H, and H<sub>2</sub> as the reactants, to reproduce a flame environment.

In the first case, benzo[*ghi*]fluoranthene and cyclopenta[*cd*]pyrene are formed from the beginning and in significant amounts. Flow analyses show that benzo[*ghi*]fluoranthene is initially formed through pathway A and as soon as H atoms are available pathway C leading to intermediates **8** and **9** becomes significant. A total of 90% of intermediate **6** is formed through the reaction  $9 + H \rightleftharpoons 6 + H_2$ . Benzo[*ghi*]fluoranthene is produced through pathways A, C, and B2.

A total of 65% of cyclopenta[*cd*]pyrene is produced through pathway H, while 30% comes from pathway G. In these conditions, the benzyne mechanism (pathway D) is not significant.

In a H-rich environment, benzo[*c*]phenanthrene pyrolysis gives predominantly benzo[*ghi*]fluoranthene, suggesting that benzo[*ghi*]fluoranthene is the primary pentacyclic PAH formed. Cyclopenta[*cd*]pyrene is formed later by the 6/5-ring switch rearrangement. In fact, after reaching a maximum, the concentration profile of benzo[*ghi*]fluoranthene decreases when cyclopenta[*cd*]pyrene starts forming. Flow analyses show that benzo[*ghi*]fluoranthene is initially formed through pathways A and C. A total of 88% of cyclopenta[*cd*]pyrene is produced through pathway H, while 9% comes from pathway G.

The energies involved in the benzo[*ghi*]fluoranthene/cyclopenta[*cd*]pyrene reaction are significantly high, making the direct interconversion unfavored. These results are in agreement with the experimental data reported by Sarobe et al.<sup>35</sup>

Independent thermolysis of benzo[*ghi*]fluoranthene gave pyrolysates containing both benzo[*ghi*]fluoranthene and cyclo-

penta[*cd*]pyrene with a low yield of the latter ( $T = 1150$  °C, **4/10** = 97%/3%).

### Conclusions

The present study identifies possible reaction pathways connecting benzo[*c*]phenanthrene to benzo[*ghi*]fluoranthene and cyclopenta[*cd*]pyrene. For the conversion of benzo[*c*]phenanthrene to benzo[*ghi*]fluoranthene, the first route involves H elimination to form radical **2**, followed by rapid cyclization to intermediate **3** and further H elimination to yield benzo[*ghi*]fluoranthene. The second pathway consists of scrambling of hydrogen atoms: first the 1,2-shift of hydrogen to produce compound **5** followed by the hydrogen 1,5-shift to produce benzo[*ghi*]fluoranthene. The third route is represented by an electrocyclic reaction which is a type of pericyclic chemical reaction where the net result is one  $\pi$ -bond being converted into one  $\sigma$ -bond. The reaction proceeds by way of a cyclic transition state, and one  $\sigma$ -bond is formed (intermediate **9**) during the course of the reaction (pathway C).

Cyclopenta[*cd*]pyrene is formed through dehydrogenation of intermediate **2** to form the corresponding benzyne benzenologue. The transient carbene is trapped via an intramolecular C–H insertion, giving the cyclopentafused product.

For the conversion of benzo[*ghi*]fluoranthene to cyclopenta[*cd*]pyrene, four different mechanisms have been identified. The first two rearrangement pathways involve the formation of four-centered reactions: the direct ring-contraction/ring-expansion mechanisms show significant energy barriers (around 160 kcal/mol, in both cases). The other two routes are promoted by H atoms, and cyclopenta[*cd*]pyrene is formed through 5/6-ring interconversion. Reaction rates and thermodynamic properties have been computed for all the species involved in the pathways.

Kinetic simulation results in a high-temperature pyrolysis environment show that benzo[*c*]phenanthrene gives benzo[*ghi*]fluoranthene through the formation of intermediates **2** and **3**. Cyclopenta[*cd*]pyrene is formed by the 6/5-ring switch rearrangement aided by H atoms. In a H-rich environment, where a radical chain mechanism can play a role, cyclopenta[*cd*]pyrene is formed from benzo[*ghi*]fluoranthene through 5/6-ring interconversion (pathway H).

These results provide an important context for the study of much larger PAHs, fullerenes, nanoparticles, and soot. During combustion processes, the formation of high-molecular-mass structures, such as nanoparticles, and their conversion to mature soot aggregates is the result of a carbonization process involving formation of activated complexes, molecular rearrangement, polymerization, and dehydrogenation.<sup>60,61</sup> Cyclodehydrogenation

reactions are responsible for the surface rearrangements of carbonaceous particles and their reactivity, and they need to be included in model descriptions for soot growth.

**Acknowledgment.** This research is funded by a National Science Foundation Collaborative Proposal (CTS-0210061). The calculations presented in this paper were carried out at the Utah Center for High Performance Computing (CHPC), University of Utah, which is acknowledged for computer time support. I am grateful to Prof. L. T. Scott and Dr. N. D. Marsh for their helpful discussions.

## References and Notes

- Plummer, B. F.; Steffen, L. K.; Herndon, W. C. *Struct. Chem.* **1993**, *4*, 279.
- Marr, J. A.; Giovane, L. M.; Longwell, J. P.; Howard, J. B.; Lafleur, A. L. *Combust. Sci. Technol.* **1994**, *101*, 301.
- Lam, F. W.; Howard, J. B.; Longwell, J. P. *Chem. Phys. Processes Combust.* **1987**, *93*, 1.
- Plummer, B. F.; Singleton, S. F. *J. Phys. Chem.* **1990**, *94*, 7363.
- Plummer, B. F.; Al-Saigh, Z. Y.; Arfan, M. *Chem. Phys. Lett.* **1984**, *104*, 389–392.
- Lowe, J. P.; Silverman, B. D. *Acc. Chem. Res.* **1984**, *17*, 332.
- Howard, J. B.; Longwell, J. P.; Marr, J. A.; Pope, C. J.; Busby, W. F.; Lafleur, A. L.; Taghizadeh, K. *Combust. Flame* **1995**, *101* (3), 262.
- Ball, L. M.; Warren, S. H.; Sangaiah, R.; Nesnow, S.; Gold, A. *Mutat. Res.* **1989**, *224*, 115.
- Durant, J. L.; Busby, W. F.; Lafleur, A. L.; Penman, B. W.; Crespi, C. L. *Mutat. Res.* **1996**, *371*, 123.
- Scott, L. T.; Roelofs, N. H. *J. Am. Chem. Soc.* **1987**, *109* (18), 5461.
- DasGupta, A.; DasGupta, N. K. *Can. J. Chem.* **1976**, *54* (20), 3227.
- Marsh, N. D.; Mikolajczak, C. J.; Wornat, M. J. *Spectrochim. Acta, Part A* **2000**, *56*, 1499.
- Scott, L. T.; Cheng, P.-C.; Hashemi, M. M.; Bratcher, M. S.; Meyer, D. T.; Warren, H. B. *J. Am. Chem. Soc.* **1997**, *119*, 10963.
- Clayton, M. D.; Rabideau, P. W. *Tetrahedron Lett.* **1997**, *38*, 741.
- Hagen, S.; Bratcher, M. S.; Erickson, M. S.; Zimmermann, G.; Scott, L. T. *Angew. Chem., Int. Ed. Engl.* **1997**, *36*, 406.
- Mehta, G.; Panda, G. *Tetrahedron Lett.* **1997**, *38*, 2145.
- Cioslowski, J.; Schimeczek, M.; Piskorz, P.; Moncrieff, D. *J. Am. Chem. Soc.* **1999**, *121*, 3773.
- Lafleur, A. L.; Howard, J. B.; Plummer, E.; Taghizadeh, K.; Necula, A.; Scott, L. T.; Swallow, K. C. *Polycyclic Aromat. Compd.* **1998**, *12* (4), 223.
- Wornat, M. J.; Sarofim, A. F.; Lafleur, A. L. *Proc. Combust. Inst.* **1992**, *24*, 955.
- Wornat, M. J.; Vriesendorp, F. J. J.; Lafleur, A. L.; Plummer, E. F.; Necula, A.; Scott, L. T. *Polycyclic Aromat. Compd.* **1999**, *13* (3), 221.
- Mukherjee, J.; Sarofim, A. F.; Longwell, J. P. *Combust. Flame* **1994**, *96*(3), 191.
- Marsh, N. D.; Zhu, D.; Wornat, M. J. *Proc. Combust. Inst.* **1998**, *27*, 1897.
- Marsh, N. D.; Wornat, M. J.; Scott, L. T.; Necula, A.; Lafleur, A. L.; Plummer, E. F. *Polycyclic Aromat. Compd.* **2000**, *13* (4), 379.
- Lafleur, A. L.; Taghizadeh, K.; Howard, J. B.; Anacleto, J. F.; Quilliam, M. A. *J. Am. Soc. Mass Spectrom.* **1996**, *7* (3), 276.
- Wornat, M. J.; Vernaglia, B. A.; Lafleur, A. L.; Plummer, E. F.; Taghizadeh, K.; Nelson, P. F.; Li, C.-Z.; Necula, A.; Scott, L. T. *Proc. Combust. Inst.* **1998**, *27*, 1677.
- Badger, G. M.; Spotswood, T. M. *J. Chem. Soc.* **1960**, 4420.
- Badger, G. M.; Jolad, S. D.; Spotswood, T. M. *Aust. J. Chem.* **1964**, *17*, 771.
- Cioslowski, J.; Liu, G.; Martinov, M.; Piskorz, P.; Moncrieff, D. *J. Am. Chem. Soc.* **1996**, *118*, 5261.
- Ebert, L. B. *Science* **1990**, *247*, 1468.
- Kroto, H. W.; McKay, K. *Nature* **1988**, *331*, 328.
- Jenneskens, L. W.; Sarobe, M.; Zwikker, J. W. *Pure Appl. Chem.* **1996**, *68*, 219 and references therein.
- Scott, L. T. *Pure Appl. Chem.* **1996**, *68*, 291 and references therein.
- Crowley, C.; Kroto, H. W.; Taylor, R.; Walton, D. R. M.; Bratcher, M. S.; Cheng, P.-C.; Scott, L. T. *Tetrahedron Lett.* **1995**, *36*, 9215.
- Lafleur, A.; Gagel, J. J.; Longwell, J. P.; Monchamp, P. A. *Energy Fuels* **1988**, *2*, 709.
- Brown, R. F. C.; Eastwood, F. W. *Pure Appl. Chem.* **1996**, *68*, 261.
- Brown, R. F. C.; Eastwood, F. W.; Harrington, K. J.; McMullen, G. L. *Aust. J. Chem.* **1974**, *27*, 2393.
- Sarobe, M.; Jenneskens, L. W.; Wiersum, U. E. *Tetrahedron Lett.* **1996**, *37*, 1121.
- Sarobe, M.; Zwikker, J. W.; Snoeijer, J. D.; Wiersum, U. E.; Jenneskens, L. W. *J. Chem. Soc., Chem. Commun.* **1994**, 89.
- Brown, R. F. C.; Eastwood, F. W.; Jackman, G. P. *Aust. J. Chem.* **1977**, *30*, 1757.
- Sarobe, M.; Snoeijer, J. D.; Jenneskens, L. W.; Slagt, M. Q.; Zwikker, J. W. *Tetrahedron Lett.* **1995**, *36*, 8489.
- Cioslowski, J.; Piskorz, P.; Moncrieff, D. *J. Org. Chem.* **1998**, *63*, 4051.
- Gaussian G03, Revision B.02: Frisch, M. J., et al., Gaussian, Inc., Pittsburgh, PA, 2003.
- Berkowitz, J.; Ellison, G. B.; Gutman, D. *J. Phys. Chem.* **1994**, *98*, 2744.
- Davico, G. E.; Bierbaum, V. M.; DePuy, C. H.; Ellison, G. B.; Squires, R. R. *J. Am. Chem. Soc.* **1995**, *117*, 2590.
- Cioslowski, J.; Piskorz, P.; Moncrieff, D. *J. Am. Chem. Soc.* **1998**, *120*, 1695.
- Wenthold, P. G.; Squires, R. R. *J. Am. Chem. Soc.* **1994**, *116*, 6401 and references therein.
- Brooks, M. A.; Scott, L. T. *J. Am. Chem. Soc.* **1999**, *121*, 5444.
- Chen, R. H.; Kafafi, S. A.; Stein, S. E. *J. Am. Chem. Soc.* **1989**, *111*, 1418.
- Burton, N. A.; Quelch, G. E.; Gallo, M. M.; Schaefer, H. F., III. *J. Am. Chem. Soc.* **1991**, *113*, 764.
- Bettinger, H. F.; Jakobson B. I.; Scuseria G. E. *J. Am. Chem. Soc.* **2003**, *125*, 5572.
- Zimmermann, G. *Eur. J. Org. Chem.* **2001**, 457.
- Alder R. W.; Harvey J. N. *J. Am. Chem. Soc.* **2004**, *126*, 2490.
- Scott, L. T.; Necula, A. *Tetrahedron Lett.* **1997**, *38*, 1877.
- Sarobe, M.; Jenneskens, L. W.; Wesseling, J.; Wiersum, U. E. *J. Chem. Soc., Perkin Trans.* **1997**, *2*, 703.
- Ducan, W. T.; Bell, R. L.; Truong, T. N. *J. Comput. Chem.* **1998**, *19*, 1039.
- Truong, T. N.; Truhlar, D. G. *J. Chem. Phys.* **1990**, *93*, 1761.
- Lutz, A. E.; Kee, R. J.; Miller, J. A. *SENKIN: a Fortran program for predicting homogeneous gas phase chemical kinetics with sensitivity analysis*; Sandia National Laboratories Report No. SAND-87-8248; Sandia National Laboratories: Albuquerque, NM, 1988.
- Kee, R. J.; Rupley, F. M.; Miller, J. A. *Chemkin II: A Fortran Chemical Kinetics Package for the analysis of gas-phase chemical kinetics*; Sandia National Laboratories Report No. SAND-89-8009B; Sandia National Laboratories: Albuquerque, NM, 1989.
- Moiseeva, N. F. *Thermochim. Acta* **1990**, *168*, 179.
- Lewis, I. C. *Carbon* **1982**, *20*, 519.
- Dobbins, R. A.; Govatzidakis, G. J.; Lu, W.; Schwartzman, A. F.; Fletcher, R. A. *Combust. Sci. Technol.* **1996**, *121*, 103.